# A Stable Lipid/TiO$_2$ Interface with Headgroup-Inversed Phosphocholine and a Comparison with SiO$_2$

Feng Wang and Juewen Liu*

Department of Chemistry, Waterloo Institute for Nanotechnology, University of Waterloo, Waterloo, Ontario N2L 3G1, Canada

**S** *Supporting Information*

**ABSTRACT:** Zwitterionic phosphocholine (PC) lipids are highly biocompatible, representing a major component of the cell membrane. A simple mixing of PC liposomes and silica (SiO$_2$) surface results in liposome fusion with the surface and formation of supported lipid bilayers. However, the stability of this bilayer is relatively low because adsorption is based mainly on weak van der Waals force. PC lipids strongly adsorb by TiO$_2$ via chemical bonding with the lipid phosphate. The lack of fusion on TiO$_2$ is attributable to the steric effect from the choline group in PC. In this study, inverse phosphocholine lipids (CP) are used, directly exposing the phosphate. Using a calcein leakage assay and cryo-TEM, fusion of CP liposome with TiO$_2$ is demonstrated. The stability of this supported bilayer is significantly higher than that of the PC/SiO$_2$ system, as indicated by washing the membrane under harsh conditions. Adsorption of CP liposomes by TiO$_2$ is inhibited at high pH. Interestingly, the CP liposome cannot fuse with silica surface because of a strong charge repulsion. This study demonstrates an interesting interplay between a soft matter surface and metal oxides. By tuning the lipid structure, it is possible to rationally control the interaction force. This study provides an alternative system for forming stable supported bilayers on TiO$_2$, and represents the first example of interfacing inverse lipids with inorganic surfaces.
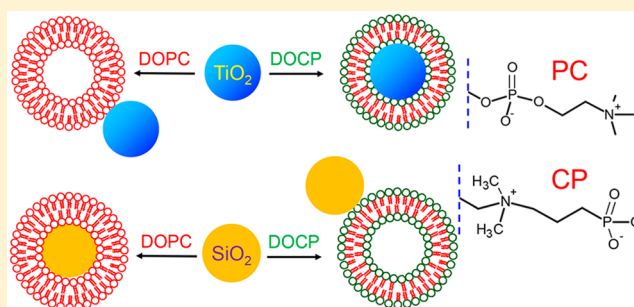
## INTRODUCTION

A stable lipid bilayer supported on a solid surface is important for a number of applications such as lipid patterning, device fabrication, and fundamental biophysical studies.[1−5] Phosphocholine (PC) lipids deposited on silica (SiO$_2$) is the most commonly used system because PC liposomes readily fuse with silica under physiological conditions.[6−11] In addition, PC liposomes are zwitterionic and highly biocompatible. A thin water layer (∼1 nm) separates the PC headgroup from the silica surface to achieve a mobile bilayer.[12,13] The PC headgroup interacts with silica surface via weak van der Waals force, resulting in a quite fragile interface that can be easily washed off.[14] For applications that require more robust films, other types of interfacial chemistry needs to be explored.[15−19]

It is interesting to note that PC liposomes do not readily fuse with many other types of surfaces, including Fe$_3$O$_4$, TiO$_2$, and highly oxidized graphene oxide.[20,21] Instead, the liposomes are stably adsorbed by these surfaces.[22−24] Similar to silica, titania (TiO$_2$) is also a highly biocompatible material.[25] A number of previous studies investigated the interaction between liposomes and TiO$_2$ surfaces, where both liposome fusion and simple adsorption were reported depending on the lipid composition.[26−35] It needs to be noted that fusion takes place with negatively charged phosphatidylserine (PS) lipids in the presence of Ca$^{2+}$, whereas liposomes composed solely of zwitterionic phospholipids only undergo adsorption under physiological conditions. Some work reported planar zwitter-

ionic bilayers on TiO$_2$ under acidic conditions.[28,34] We recently showed that TiO$_2$ can tightly adsorb PC liposomes because of the lipid phosphate interacting directly with the TiO$_2$ surface, forming a chemical bond.[21] This interaction is much stronger compared to that with silica.

However, under our tested conditions, PC liposomes do not fuse onto the TiO$_2$ surface. This was attributed to the steric effect from the choline group that impedes formation of planar supported bilayer (Figure 1B).[21] Note that the phosphate part in the headgroup is shielded by the quandary amine. We reason that this problem might be solved by inversing the headgroup dipole to directly expose the phosphate. This way, the zwitterionic nature of the lipid is still maintained, whereas the surface interaction might be enhanced (Figure 1C). One such lipid is 2-((2,3-bis(oleoyloxy)propyl)dimethylammonio)ethyl hydrogen phosphate (DOCP).[36] DOCP was first reported by the Szoka group, and this inverse headgroup chemistry has been used for drug delivery applications.[37−39] In this work, we study its interaction with TiO$_2$. By comparing 1,2-dioleoyl-*sn*-glycero-3-phosphocholine (DOPC) and DOCP, new fundamental insights were obtained. To have a full understanding, SiO$_2$ was also used. Our results indicate that supported bilayers can form with DOCP/TiO$_2$ and with DOPC/SiO$_2$ but not the
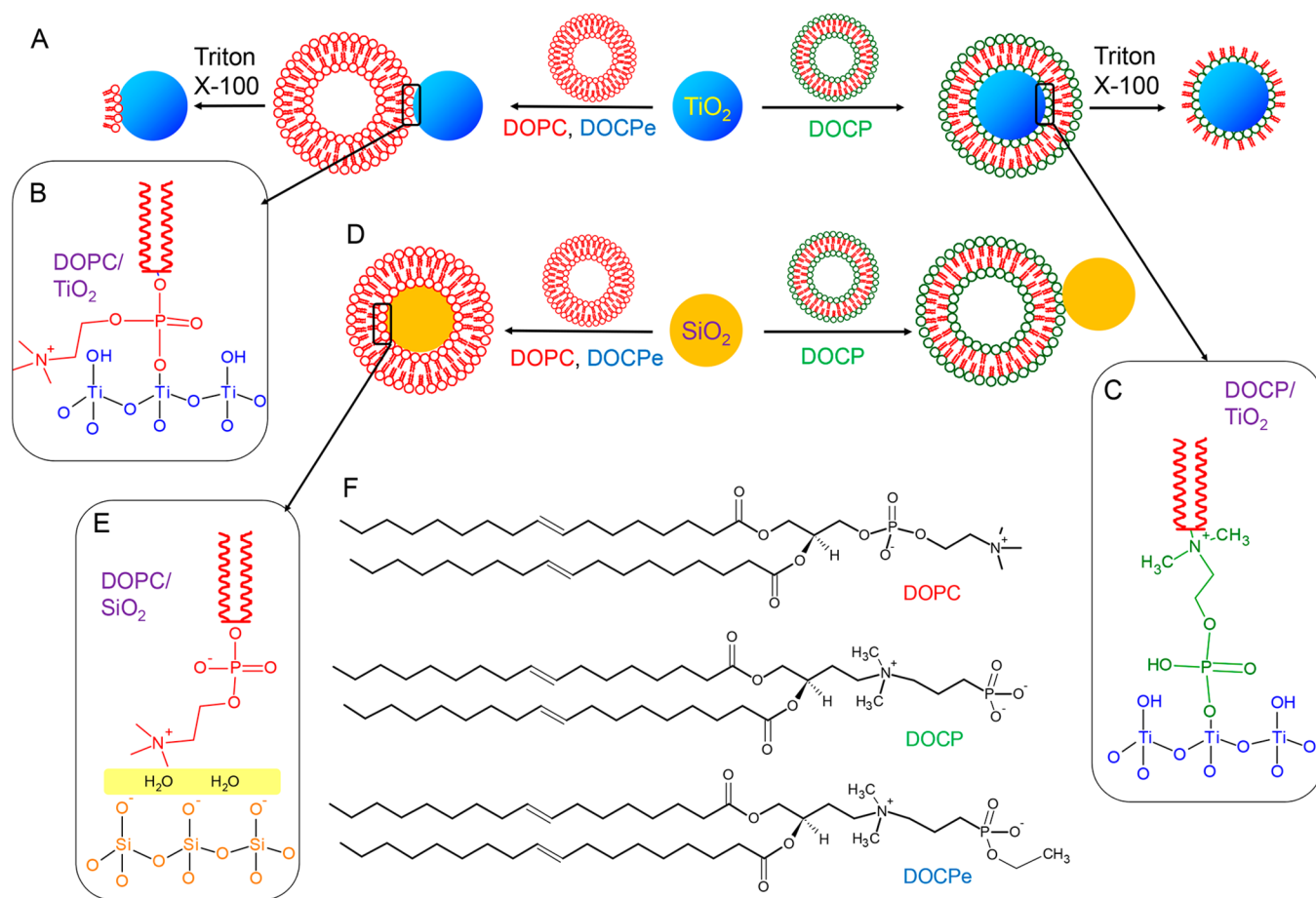
**Figure 1.** (A) Schematics of DOPC liposome adsorption by $TiO_2$ NPs and DOCP liposome forming supported bilayers. The effect of washing by Triton X-100 is also compared. (B) DOPC/$TiO_2$ interface chemistry. The steric effect from the choline group in DOPC might be the cause of liposome fusion inhibition. (C) DOCP/$TiO_2$ interface, where the steric effect is alleviated. (D) Interactions of these liposomes with $SiO_2$ NPs is completely reversed. (E) DOPC/$SiO_2$ interface. A thin water layer separates the two surfaces, and adsorption is achieved by van der Waals force. (F) Structures of DOPC, DOCP, and DOCPe lipids.

other way around. This also represents the first example of interfacing inverse lipids with inorganic materials surfaces.

## ■ MATERIALS AND METHODS

**Chemicals.** All the phospholipids were purchased from Avanti Polar Lipids (Alabaster, AL). $SiO_2$ nanoparticles (NPs) in aqueous suspension (50 nm, 5.73 wt %) were from Polyscience Inc. (Warrington, PA). Disodium calcein, choline chloride, Triton X-100, and 20 nm $TiO_2$ NPs (catalog number 718467) were from Sigma-Aldrich. $TiO_2$ NPs (50 nm, US3530, and 500 nm, US3548) were from US Research nanomaterials (Houston, TX). 4-(2-hydroxyethyl)-1-piperazineethanesulfonic acid (HEPES) and NaCl were from Mandel Scientific (Guelph, ON, Canada). Milli-Q water was used to prepare all the buffers and solutions. All the other reagents and solvents were of analytical grade and used as received.

**Preparation of Liposomes.** Liposomes were prepared using the standard extrusion method as described previously.[40] DOPC, DOCP, and 2-((2,3-bis(oleoyloxy)propyl)dimethylammonio)ethyl ethyl phosphate (DOCPe) with a total mass of 2.5 mg were respectively dissolved in chloroform. Rh-labeled liposomes were prepared by including 1% Rh-PE (2-dioleoyl-sn-glycero-3-phosphoethanolamine-N-(lissaminerhodamine B sulfonyl) (ammonium salt) in chloroform. Chloroform was then removed under a gentle $N_2$ flow followed by storing the samples in a vacuum oven overnight at room temperature. The dried lipid films were kept under a $N_2$ environment and then stored at −20 °C prior to use. To prepare liposomes, the lipids were hydrated with 0.5 mL of buffer A (100 mM NaCl, 10 mM HEPES, pH 7.4) at room temperature with occasional sonication for at least 2 h.

Therefore, the lipid concentration was 5 mg mL$^{-1}$. The resulting cloudy suspension was extruded 21 times through two stacked polycarbonate membranes (pore size = 100 nm). To encapsulate calcein, the above prepared lipid films were hydrated with 100 mM calcein solution overnight and then extruded. Free calcein was removed by passing 50 μL of the samples through a Pd-10 column using buffer A for elution. The first 600 μL of the fluorescent fraction was collected.

**Leakage Studies.** Our $TiO_2$ NPs were soaked in NaOH (0.1 M) overnight to achieve a reproducible surface. Then, the $TiO_2$ NPs were washed extensively by Milli-Q water. To monitor NP-induced liposome leakage, 5 μL of the above purified calcein-loaded liposome solution was added to 595 μL of buffer A in a quartz cuvette at 25 or 37 °C. After 5 min, $TiO_2$ (20 nm) or $SiO_2$ NPs (6 μL, 1 mg mL$^{-1}$) were added. The fluorescence intensity was monitored for another 25 min before 10 μL of 5% Triton X-100 was added. Calcein was excited at 485 nm, and the fluorescence emission was monitored at 515 nm using a Varian Eclipse fluorometer. To study the size and concentration effect $TiO_2$ NPs, 20 nm (6 μL, 1 mg mL$^{-1}$) or 50 nm $TiO_2$ NPs (6 μL, 1 mg mL$^{-1}$ or 5 mg mL$^{-1}$) were added at 37 °C. For $SiO_2$ NPs, 10 μL of calcein-loaded DOPC, DOCP, or DOCPe liposomes were added to 200 μL of $SiO_2$ (100 μg mL$^{-1}$) and incubated for 30 min at room temperature. After centrifugation at 15 000 rpm to precipitate liposome/$SiO_2$ complexes, the supernatant was collected. The pellets were washed three times by buffer A and then dispersed in the same buffer. Then, Triton X-100 (1 μL, 5%) was added. The fluorescence intensity of these samples was documented
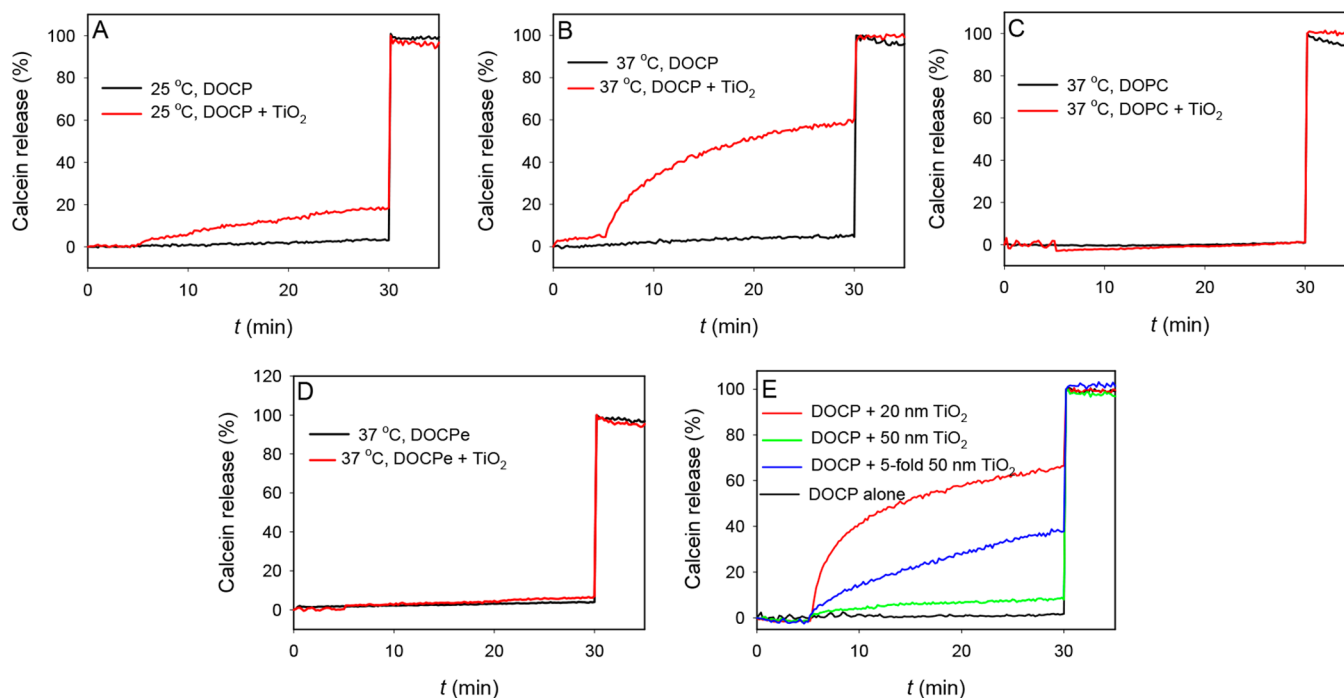
**Figure 2.** Calcein-loaded liposome fusion test when mixed with TiO$_2$ NPs. TiO$_2$ NPs (20 nm) were added to (A) DOCP at 25 °C, (B) DOCP at 37 °C, (C) DOPC at 37 °C, and (D) DOCPe at 37 °C. (E) Calcein-loaded DOCP leakage as a function of TiO$_2$ NP size and concentration. At the same mass concentration, leakage by the larger 50 nm TiO$_2$ was much less than that by the 20 nm TiO$_2$, which was attributable to the smaller surface area. By raising the concentration of 50 nm TiO$_2$, accelerated leakage is achieved. Buffer: 100 mM NaCl, 10 mM HEPES, and pH 7.4. At 5 min, TiO$_2$ NPs were added, and at 30 min, Triton X-100 was added.

by using a digital camera and a hand-held UV lamp in a dark room (Canon PowerShot SD 1200 IS).

**Liposome Adsorption Studies.** HCl was used to adjust pH from 3 to 7, and NaOH was used to adjust pH from 9 to 11. To 200 $\mu$L of NaOH-treated TiO$_2$ solution (20 nm, 200 $\mu$g mL$^{-1}$), 1 $\mu$L of Rh-labeled liposomes (5 mg mL$^{-1}$) was added and incubated for 10 min. After centrifugation at 15 000 rpm to precipitate the liposome/TiO$_2$ complexes, the supernatant fluorescence was photographed in a dark room or measured by a fluorometer. To measure the effect of salt concentration, 200 $\mu$L of TiO$_2$ (200 $\mu$g mL$^{-1}$) or SiO$_2$ (1 mg mL$^{-1}$) in water was mixed with 2 $\mu$L of Rh-labeled liposomes (5 mg mL$^{-1}$). Then, NaCl was added to designated concentrations. The amount of nonadsorbed liposomes were calculated from the supernatant fluorescence intensity after centrifugation. Rh was excited at 560 nm, and the emission fluorescence was monitored at 592 nm.

**Cryo-TEM.** NaOH-treated TiO$_2$ NPs (500 nm) were used. The TiO$_2$-supported DOCP bilayers or DOPC/TiO$_2$ were prepared with an excess amount of the liposomes (in 10 mM MES pH 6.0 with 100 mM NaCl incubated overnight), and free liposomes were removed after centrifugation and extensive washing. Cryo-TEM experiment was carried out by spotting DOPC/TiO$_2$ (5 $\mu$L) or DOCP/TiO$_2$ (5 $\mu$L) on a carbon-coated copper TEM grid (treated with plasma to ensure surface was hydrophilic) in a humidity-controlled chamber. The humidity was set to be 95−100% during this operation. The grid was blotted with two filter papers for 2 s and quickly plunged into liquid ethane. The sample was then loaded to a liquid-N$_2$-cooled cold stage and loaded into a 200 kV field emission TEM (FEI Tecnai G2 F20). The samples were imaged when the temperature was stabilized at −178 °C.

**Adsorption Stability Test.** A 1 $\mu$L aliquot of Rh-labeled DOPC, DOCP, or DOCPe liposomes (5 mg mL$^{-1}$) were mixed with 200 $\mu$L of 20 nm TiO$_2$ (200 $\mu$g mL$^{-1}$) or SiO$_2$ (1 mg mL$^{-1}$) in 100 mM NaCl and incubated for 10 min at 37 °C. After centrifugation at 15 000 rpm to precipitate the liposome/oxide hybrid, the pellets were redispersed in phosphate (100 mM); surfactant (5% triton X-100); urea (6 M), Na$^+$, Mg$^{2+}$, or NO$_3^-$ (100 mM each); pH 3 or pH 11 solution; BSA

(100 mg mL$^{-1}$) and incubated for another 15 min. The amount of released liposomes in the supernatant was quantified by fluorescence.

## RESULTS AND DISCUSSION

**Liposome Fusion onto TiO$_2$ Surface.** In this study, three types of liposomes with different headgroup structures were employed (Figure 1F). DOPC is the normal zwitterionic lipid with a net charge of zero at physiological pH. The headgroup of the inverse phosphocholine (DOCP) lipid has an exposed phosphate with two negative charges. As a result, each DOCP molecule carries one net negative charge. To remove the charge effect, DOCPe is also included, where the phosphate is capped by an ethyl group. Our liposomes were prepared using the extrusion method to yield ∼100 nm diameter liposomes. (See Figure S1 for size measured by DLS.) The much higher negative charge of DOCP is also confirmed by the zeta potential data (Figure S2).

To probe liposome fusion with nanomaterials, calcein-loaded liposomes are ideal for this purpose.[20,21] We encapsulated 100 mM calcein inside these three types of liposomes and free calcein was removed. Because the calcein concentration is very high inside the liposomes, its fluorescence is self-quenched. If the liposomes are ruptured, then calcein is released into the whole solution to enhance fluorescence. At room temperature (∼25 °C), calcein-loaded free DOCP liposomes are quite stable (Figure 2A, black trace). At 30 min, Triton X-100 was added to fully rupture the liposomes, resulting in a strong fluorescence enhancement. When mixed with TiO$_2$ NPs (20 nm), a gradual fluorescence increase was observed (Figure 2A, red curve), suggesting that the liposome was adsorbed and subsequently ruptured on the surface, forming a supported bilayer. The fluorescence increase is faster when temperature is raised to 37
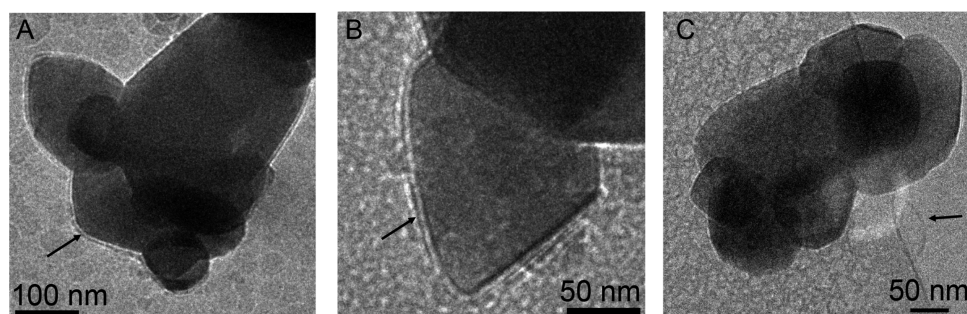
**Figure 3.** (A and B) Cryo-TEM micrographs of DOCP liposomes mixed with TiO$_2$ NPs. The arrowheads point at the lipid bilayer feature supported on TiO$_2$. (C) Cryo-TEM micrograph of DOPC liposome mixed with TiO$_2$ NPs. The arrowhead points at an intact liposome. The TiO$_2$ edge also lacks the feature of supported lipid bilayers.

°C (Figure 2B), suggesting that liposome fusion is an activated process that requires energy.

For comparison, no fluorescence enhancement was observed when TiO$_2$ NPs (20 nm) were added to calcein-loaded DOPC even at 37 °C (Figure 2C), consistent with our previous study.[21] We propose that the phosphate group in the lipid molecule is the main contributor to the adsorption. The strong chemical interaction between titanium and phosphate has been well documented.[41−44] However, the choline group in DOPC imposes a strong steric hindrance to inhibit full liposome fusion. (See Figure 1B for the steric effect.) It is interesting to note that DOCPe also failed to produce fluorescence enhancement (Figure 2D). Therefore, this small ethyl cap also inhibited the fusion reaction. From this simple study, we already observed the significant effect of inversing the headgroup of the DOPC lipid and having a fully exposed phosphate group. This comparison is summarized in Figure 1A.

Aside from the inversed dipole, another difference between DOPC and DOCP is the extra negative charge, so here we also discuss the charge effect. Under our experimental condition of pH 7.4, the surface of TiO$_2$ is negatively charged (Figure S3). DOCP also carries a negative charge. Therefore, the electrostatic interaction between TiO$_2$ and DOCP is repulsive, and the fusion between them cannot be explained by electrostatic attraction. The fact that DOCP can fuse with TiO$_2$ strongly indicates the importance of the exposed phosphate group.

We next studied the size or curvature effect of TiO$_2$ NPs (Figure 2E). All the previous assays used 20 nm TiO$_2$. When 50 nm TiO$_2$ was used at the same mass concentration, the calcein leakage rate was significantly slower (Figure 2E, green trace). This might be attributable to the smaller surface area of larger NPs. When the concentration of the 50 nm NPs was raised fivefold so that the surface area became comparable with that of the 20 nm sample, we then observed much faster calcein leakage. This study indicates that DOCP fusion with TiO$_2$ can occur with both small and large TiO$_2$ NPs.

**Supported DOCP Bilayers Characterized by Cryo-TEM.** The above calcein leakage tests suggest DOCP liposome fusion with TiO$_2$, but we cannot rule out local defects or pores on the liposome induced by TiO$_2$. To further confirm formation of supported bilayers, we carried out cryo-TEM studies. The TiO$_2$ NPs were mixed with DOCP liposomes, and the free liposomes were washed away. In this study, we used larger TiO$_2$ NPs because smaller ones tend to aggregate, which may mask the supported bilayer features.[21] The samples were then quickly vitrified in liquid ethane and imaged. The TiO$_2$ surface is clearly wrapped by a lipid bilayer (Figure 3A,B), consistent with the known lipid fusion mechanism. Our

previous work showed that when DOPC liposomes were mixed with TiO$_2$ NPs the liposomes remain spherical and are only adsorbed without fusion. (The lack of calcein leakage also supports stable adsorption.)[21] Here we repeated the experiment with the larger TiO$_2$ NPs, and intact DOPC adsorption was also observed (Figure 3C). In this sample, the TiO$_2$ surface lacks the bilayer structure observed in Figure 3A,B, further supporting the scheme in Figure 1A. This experiment confirms the importance of the structural difference between DOPC and DOCP, yielding different hybrid materials with TiO$_2$.

**Bilayer Stability Comparison.** By combining the cryo-TEM and calcein leakage data, we confirmed that DOCP formed supported bilayers on TiO$_2$. An important motivation to use TiO$_2$ is to enhance bilayer stability. For many applications, it is important to have a stable lipid layer, such as in a flow channel.[45−47] Therefore, we challenged our system with various chemicals that might be encountered under harsh conditions. These chemicals can also probe lipid adsorption mechanisms. To track lipid molecules, we labeled these liposomes with 1% Rh-PE (a rhodamine-modified headgroup). The liposomes were mixed with 20 nm TiO$_2$ NPs, and free liposomes were removed. Then, various chemicals were added, and the samples were centrifuged to precipitate the TiO$_2$/liposome hybrids. The fluorescence intensity in the supernatant is thus proportional to the lipids that are washed away by the treatments. A total of four systems were compared. The most important comparison is between DOCP/TiO$_2$ (black bars, Figure 4) and DOPC/SiO$_2$ (red bars). In all the cases, especially with high pH, urea, surfactant, and proteins, the DOCP/TiO$_2$ system showed much higher stability. In other cases, both systems are quite stable. Therefore, the inverse lipid
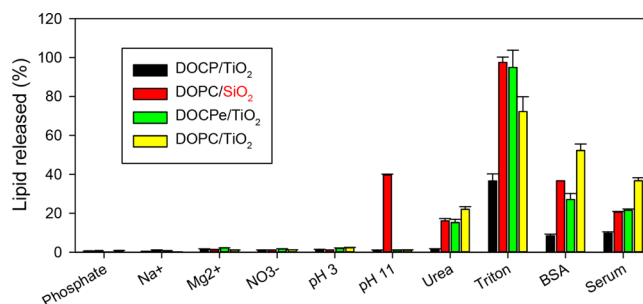


**Figure 4.** Displacement of adsorbed DOPC, DOCP, or DOCPe liposomes from TiO$_2$ by ions (e.g., phosphate, Na$^+$, Mg$^{2+}$, and NO$_3^-$; 100 mM each), extreme pH (3 and 11), hydrogen-bond breaker (urea, 6 M), surfactant (5% triton X-100), and proteins (100 mg mL$^{-1}$).
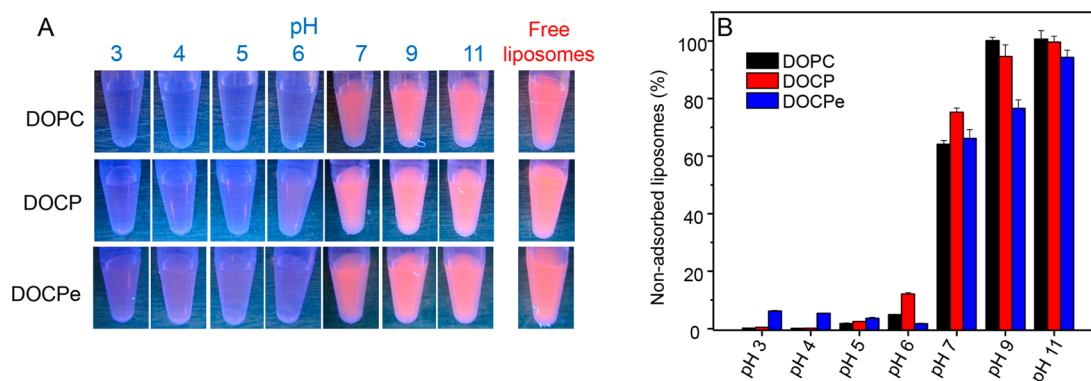
**Figure 5.** (A) Photographs of the supernatants of the Rh-labeled DOPC, DOCP, and DOCPe liposomes mixing with TiO$_2$ NPs at various pH values and after centrifugation. Higher fluorescence indicates lower adsorption. (B) Quantitative analysis nonadsorbed liposomes by TiO$_2$ as a function of pH. A lower bar indicates more liposome adsorption.

and TiO$_2$ can indeed achieve a more stable supported bilayer. It needs to be pointed out that the adsorption stability of the DOPC/SiO$_2$ system might be higher in our particle-supported system because the lipid can form a sealed bilayer covering the whole particle. On a planar surface, the stability might be even lower because of the exposed lipid edge,[5,48,49] whereas for the TiO$_2$ system, the planar bilayer should be also very stable because of the strong phosphate/Ti interaction.

Another comparison we make is among the three types of liposomes on TiO$_2$. Because these lipids are believed to interact via phosphate bonding, free phosphate ions were tested first. When 100 mM phosphate was added, no liposome release was observed for any of the liposomes (first set of bars in Figure 4). Therefore, once adsorbed, free phosphate cannot displace them. Other anions and cations, such as Na$^+$, Mg$^{2+}$, and nitrate, were also added. They released less than 2.5% of the lipids. To further understand the interaction mechanism, we next challenged the liposome/TiO$_2$ conjugates at pH 3 and 11, and less than 5% of DOCP was released. Therefore, electrostatic interaction is also not a main contributor for the attractive force, which is consistent with our hypothesis.

Next, we challenged the system with even harsher conditions. Urea breaks hydrogen bonds, and it is commonly used to probe molecular interactions. Interestingly, DOPC released ~20%, but DOCP barely showed any release. Note that 6 M urea was used in this study. Both samples are stable with 1 M urea (data not shown). This is an indication that both liposomes are adsorbed very strongly and that hydrogen bonding is not the main stabilizing force for the supported bilayers.

We also challenged the samples with surfactants. For DOPC, Triton X-100 released ~70% of lipid, whereas DOCP only released ~40%. Because this surfactant can disrupt bilayer structure and even dissolve individual lipid molecules, only strongly adsorbed lipids can survive this treatment. The fact that significantly less DOCP was released suggests that its inner leaflet is stably adsorbed, whereas for DOPC, only the lipids at the contacting points are stably adsorbed. (See Figure 1A for this difference after the Triton X-100 treatment.) This experiment also provides strong evidence that DOCP forms a supported bilayer (instead of monolayer) on TiO$_2$. Finally, bovine serum albumin (BSA) was added. This protein can be adsorbed by many NPs, such as silica NPs, AuNPs, and TiO$_2$. For DOPC, BSA released 52.2% lipid. However, for DOCP, only 8.4% lipid was released. In a sense, proteins are similar to surfactants (with both hydrophobic and hydrophilic domains),

and a high concentration of proteins can also dissolve a fraction of lipids. Similar observations were made with blood serum (the last set of bars). Overall, once adsorbed, all the lipids are quite stable on TiO$_2$. In particular, DOCP forms the most stable hybrid.

High lipid adsorption stability can also be achieved by using thiolated lipids on gold.[50] However, the TiO$_2$/DOCP system has a few advantages. For example, if a thiol group is modified on the lipid tail, then a monolayer is formed on gold, leaving insufficient room for applications such as transmembrane protein insertion. If a thiol group is modified on the lipid headgroup, then a supported bilayer may form on gold. However, the outer leaflet headgroup also contains the thiol, which is undesirable because the active thiol is likely to interfere with downstream applications. Although it is possible to wash away the top leaflet and then add another lipid monolayer, this becomes a very complicated operation. Our DOCP system naturally forms a bilayer by a simple mixing step.

**Adsorption as a Function of pH.** Similar to many other oxides, the surface charge of TiO$_2$ is also a strong function of pH, and pH-dependent studies can provide mechanistic insights. From the washing experiments in Figure 4, we already know that once the lipid/TiO$_2$ interface is formed, it is quite stable even under extreme pH conditions. To further study the adsorption condition, we adjusted pH before mixing the Rh-labeled liposomes with TiO$_2$ NPs. After mixing, the samples were centrifuged. Adsorbed liposomes were precipitated, and Figure 5A showed a picture of the supernatant fluorescence intensity. The intensity is quantified in Figure 5B, and adsorption is inhibited at high pH. All the liposomes showed the same trend, suggesting that the mechanism of adsorption is the same. When the TiO$_2$ surface is negatively charged at high pH, it is more difficult for the negatively charged phosphate group to perform nucleophilic attack of the Ti center. This is also true for the inverse phosphocholine liposomes DOCP and DOCPe. It needs to be re-emphasized that once formed, the lipid/TiO$_2$ complexes are quite stable and can survive high pH treatments (Figure 4).

**Interaction with SiO$_2$ NPs.** The above work is mainly focused on TiO$_2$ NPs, where the behavior between DOPC and DOCP is completely different. To have a full understanding, we also compared these liposomes using SiO$_2$ NPs. (See Figure S4 for TEM micrograph of SiO$_2$.) First, fusion was probed using calcein-loaded liposomes. All the calcein-loaded liposomes were almost nonfluorescent as expected (Figure 6A, samples in the
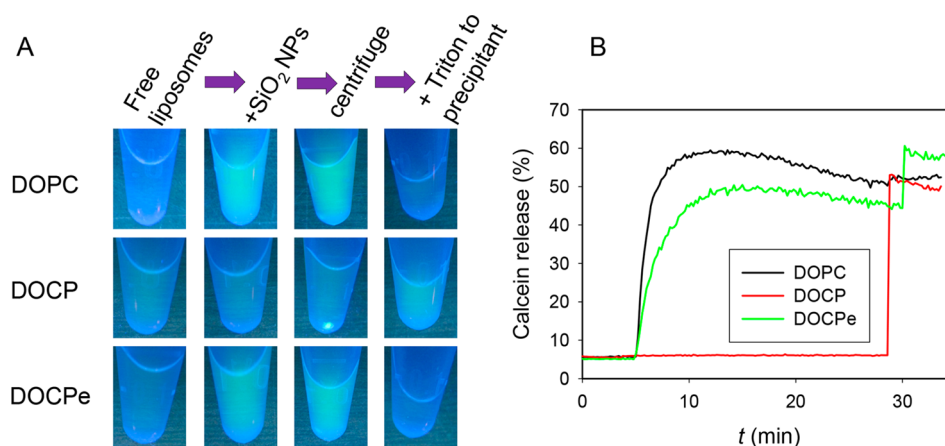
**Figure 6.** (A) Fluorescence photographs of the three calcein-loaded liposomes mixed with SiO$_2$ NPs and after various treatments. (B) Fluorescence kinetic traces showing SiO$_2$-induced leakage of DOPC and DOCPe liposomes but not the DOCP liposome. The SiO$_2$ concentration was 100 $\mu$g/mL. The experiment was carried out in 10 mM HEPES buffer, pH 7.4, with 100 mM NaCl.

first column). Addition of SiO$_2$ NPs produced strong green fluorescence for DOPC and DOCPe, suggesting rupture of the liposomes and release of the encapsulated calcein. However, no fluorescence enhancement was observed when SiO$_2$ NPs were added to the DOCP liposomes, indicating that the liposomes remained stable in this case. Then, these samples were centrifuged, and a bright pellet was observed with the DOCP sample. This spot is composed of the SiO$_2$ NPs and associated DOCP liposomes, suggesting that the liposome can be adsorbed by SiO$_2$ NPs although no subsequent fusion occurred. Finally, the pellets from the three samples were washed, and Triton X-100 was added. Only the DOCP sample produced fluorescence. This confirms DOCP were adsorbed as intact liposomes, whereas the other two liposomes both ruptured after adsorption.

We next followed the kinetics of fluorescence enhancement upon adding SiO$_2$ NPs (Figure 6B). At 5 min, SiO$_2$ NPs were added, and at ∼30 min, Triton X-100 was added. For DOPC liposomes (black trace), the fluorescence gradually increased upon SiO$_2$ addition, and full release was achieved. The rate is slightly slower for DOCPe, but close-to-full release can also be achieved. Consistent with the data in Figure 6A, no leakage was detected with DOCP. This might be related to the strong negatively charged DOCP surface. The interaction between SiO$_2$ and these three liposomes is summarized in Figure 1D.

**Adsorption of the Liposomes by SiO$_2$ NPs.** To understand the difference observed in Figure 6, we studied the adsorption of these liposomes by SiO$_2$ NPs. Because silica is negatively charged (zeta potential = −20 mV at pH 7.4) and the liposomes are either negatively charged or charge neutral, we suspect that salt concentration is important for modulating long-ranged electrostatic interactions. Using Rh-labeled liposomes, we quantified adsorption capacity after centrifugation as a function of NaCl concentration (Figure 7). DOPC has little adsorption in the absence of salt, and efficient adsorption is achieved with just 10 mM NaCl, suggesting a mild repulsion that can be efficiently screened with a low concentration of salt. DOCP, in contrast, required more than 100 mM NaCl to achieve efficient adsorption, whereas DOCPe stands in between, showing high adsorption capacity with more than 30 mM NaCl. The Debye lengths are ∼3.0 nm (10 mM NaCl), 1.8 nm (30 mM NaCl), and 0.95 nm (100 mM NaCl) in these salt concentrations. This electrostatic screen length reflects the
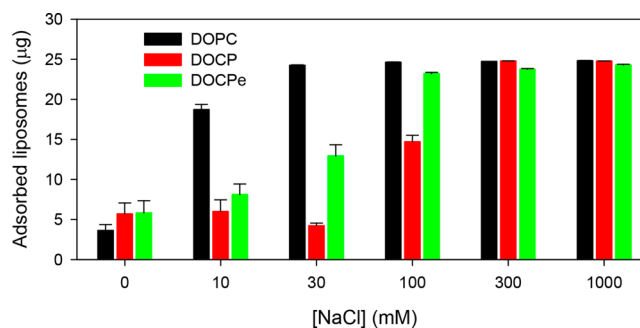


**Figure 7.** Mass of the three types of Rh-labeled liposomes associated with 100 $\mu$g of SiO$_2$ NPs as a function of NaCl concentration at pH 7.4.

microscopic picture of the liposomes approaching the SiO$_2$ surface. Van der Waals force is the main attractive force responsible for liposome adsorption by SiO$_2$.[12,48,51] More negatively charged liposomes need to approach the SiO$_2$ surface even more closely to allow the van der Waals force to dominate over charge repulsion. This trend agrees with the charging property of the lipids as measured by the zeta potential. We reason that the lack of DOCP fusion on SiO$_2$ NP is related to the stronger charge repulsion that prevents extensive contact between these two surfaces.

## CONCLUSIONS

We systematically compared the adsorption of three types of zwitterionic liposomes with SiO$_2$ and TiO$_2$ NPs. The phosphate groups in these lipids directly bond to the TiO$_2$ surface, forming strong chemical interactions. All these three liposomes can be stably adsorbed by TiO$_2$. Fusion is observed only with DOCP, and we propose that the other two suffer from steric repulsion. In contrast, SiO$_2$ interacts with the liposomes mainly via weak van der Waals interaction, and fusion with DOCP is hindered by charge repulsion when the phosphate group carries two negative charges. Overall, adsorption by TiO$_2$ is much stronger than that by SiO$_2$. This study has revealed new insights into the soft/nano materials interface, and the resulting hybrid materials might be useful for biophysical, biomedical, and analytical applications. Artificial lipids such as DOCP can serve as very useful probes for

fundamental physical studies as well as reagents for making stable biointerfaces.

## ASSOCIATED CONTENT

### Supporting Information

The Supporting Information is available free of charge on the ACS Publications website at DOI: 10.1021/jacs.5b06642.

   DLS data on liposomes and nanoparticles used in this work and TEM of SiO$_2$ NPs. (PDF)

## AUTHOR INFORMATION

### Corresponding Author

*liujw@uwaterloo.ca

### Notes

The authors declare no competing financial interest.

## ACKNOWLEDGMENTS

## REFERENCES

(1) Sackmann, E. *Science* **1996**, *271*, 43.
(2) Sackmann, E.; Tanaka, M. *Trends Biotechnol.* **2000**, *18*, 58.
(3) Castellana, E. T.; Cremer, P. S. *Surf. Sci. Rep.* **2006**, *61*, 429.
(4) Parikh, A. N.; Groves, J. T. *MRS Bull.* **2006**, *31*, 507.
(5) Troutier, A.-L.; Ladavière, C. *Adv. Colloid Interface Sci.* **2007**, *133*, 1.
(6) Yee, C. K.; Amweg, M. L.; Parikh, A. N. *J. Am. Chem. Soc.* **2004**, *126*, 13962.
(7) Jung, H.; Robison, A. D.; Cremer, P. S. *J. Am. Chem. Soc.* **2009**, *131*, 1006.
(8) Liu, J.; Stace-Naughton, A.; Jiang, X.; Brinker, C. J. *J. Am. Chem. Soc.* **2009**, *131*, 1354.
(9) Yamazaki, V.; Sirenko, O.; Schafer, R. J.; Groves, J. T. *J. Am. Chem. Soc.* **2005**, *127*, 2826.
(10) Groves, J. T.; Ulman, N.; Boxer, S. G. *Science* **1997**, *275*, 651.
(11) Gopalakrishnan, G.; Rouiller, I.; Colman, D. R.; Lennox, R. B. *Langmuir* **2009**, *25*, 5455.
(12) Cremer, P. S.; Boxer, S. G. *J. Phys. Chem. B* **1999**, *103*, 2554.
(13) Kim, J.; Kim, G.; Cremer, P. S. *Langmuir* **2001**, *17*, 7255.
(14) Richter, R. P.; Brisson, A. R. *Biophys. J.* **2005**, *88*, 3422.
(15) Daniel, S.; Albertorio, F.; Cremer, P. S. *MRS Bull.* **2006**, *31*, 536.
(16) Gao, W.; Hu, C.-M. J.; Fang, R. H.; Zhang, L. *J. Mater. Chem. B* **2013**, *1*, 6569.
(17) Hartman, K. L.; Kim, S.; Kim, K.; Nam, J.-M. *Nanoscale* **2015**, *7*, 66.
(18) Tan, S.; Li, X.; Guo, Y.; Zhang, Z. *Nanoscale* **2013**, *5*, 860.
(19) Verma, A.; Stellacci, F. *Small* **2010**, *6*, 12.
(20) Ip, A. C. F.; Liu, B.; Huang, P.-J. J.; Liu, J. *Small* **2013**, *9*, 1030.
(21) Wang, F.; Liu, J. *Small* **2014**, *10*, 3927.
(22) Yu, Y.; Anthony, S. M.; Zhang, L. F.; Bae, S. C.; Granick, S. *J. Phys. Chem. C* **2007**, *111*, 8233.
(23) Zhang, L. F.; Granick, S. *Nano Lett.* **2006**, *6*, 694.
(24) Wang, B.; Zhang, L. F.; Bae, S. C.; Granick, S. *Proc. Natl. Acad. Sci. U. S. A.* **2008**, *105*, 18171.
(25) Kokubo, T.; Kim, H. M.; Kawashita, M. *Biomaterials* **2003**, *24*, 2161.
(26) Reviakine, I.; Rossetti, F. F.; Morozov, A. N.; Textor, M. *J. Chem. Phys.* **2005**, *122*, 204711.
(27) Tero, R.; Ujihara, T.; Urisu, T. *Langmuir* **2008**, *24*, 11567.
(28) Cho, N. J.; Frank, C. W. *Langmuir* **2010**, *26*, 15706.
(29) Keller, C. A.; Glasmastar, K.; Zhdanov, V. P.; Kasemo, B. *Phys. Rev. Lett.* **2000**, *84*, 5443.
(30) Rossetti, F. F.; Textor, M.; Reviakine, I. *Langmuir* **2006**, *22*, 3467.
(31) Rossetti, F. F.; Bally, M.; Michel, R.; Textor, M.; Reviakine, I. *Langmuir* **2005**, *21*, 6443.
(32) Khan, T.; Grandin, H. M.; Mashaghi, A.; Textor, M.; Reimhult, E.; Reviakine, I. *Biointerphases* **2008**, *3*, FA90.
(33) Scott, M. J.; Jones, M. N. *Colloids Surf., A* **2002**, *207*, 69.
(34) Cho, N.-J.; Jackman, J. A.; Liu, M.; Frank, C. W. *Langmuir* **2011**, *27*, 3739.
(35) Reimhult, E.; Hook, F.; Kasemo, B. *Langmuir* **2003**, *19*, 1681.
(36) Perttu, E. K.; Kohli, A. G.; Szoka, F. C. *J. Am. Chem. Soc.* **2012**, *134*, 4485.
(37) Motion, J. P. M.; Nguyen, J.; Szoka, F. C. *Angew. Chem., Int. Ed.* **2012**, *51*, 9047.
(38) Yu, X.; Liu, Z.; Janzen, J.; Chafeeva, I.; Horte, S.; Chen, W.; Kainthan, R. K.; Kizhakkedathu, J. N.; Brooks, D. E. *Nat. Mater.* **2012**, *11*, 468.
(39) Yu, X.; Yang, X.; Horte, S.; Kizhakkedathu, J. N.; Brooks, D. E. *Biomaterials* **2014**, *35*, 278.
(40) Dave, N.; Liu, J. *ACS Nano* **2011**, *5*, 1304.
(41) Ikeguchi, Y.; Nakamura, H. *Anal. Sci.* **1999**, *15*, 229.
(42) Chen, C.-T.; Chen, Y.-C. *Anal. Chem.* **2005**, *77*, 5912.
(43) Zhou, H.; Ye, M.; Dong, J.; Han, G.; Jiang, X.; Wu, R.; Zou, H. *J. Proteome Res.* **2008**, *7*, 3957.
(44) Zhang, X.; Wang, F.; Liu, B.; Kelly, E. Y.; Servos, M. R.; Liu, J. *Langmuir* **2014**, *30*, 839.
(45) Liu, C.; Monson, C. F.; Yang, T.; Pace, H.; Cremer, P. S. *Anal. Chem.* **2011**, *83*, 7876.
(46) Liu, C.; Huang, D.; Yang, T.; Cremer, P. S. *Anal. Chem.* **2014**, *86*, 1753.
(47) Yang, T. L.; Jung, S. Y.; Mao, H. B.; Cremer, P. S. *Anal. Chem.* **2001**, *73*, 165.
(48) Orozco-Alcaraz, R.; Kuhl, T. L. *Langmuir* **2013**, *29*, 337.
(49) Weirich, K. L.; Israelachvili, J. N.; Fygenson, D. K. *Biophys. J.* **2010**, *98*, 85.
(50) Sun, W.; Kewalramani, S.; Hujsak, K.; Zhang, H.; Bedzyk, M. J.; Dravid, V. P.; Thaxton, C. S. *Langmuir* **2015**, *31*, 3232.
(51) Anderson, T. H.; Min, Y.; Weirich, K. L.; Zeng, H.; Fygenson, D.; Israelachvili, J. N. *Langmuir* **2009**, *25*, 6997.